Bulletin of the JSME Vol.17, No.6, 2023
Journal of Advanced Mechanical Design, Systems, and Manufacturing

Development of the spindle shaft for machining center using high thermal conductivity material

Shingo KAJIKAWA*, Sho MORITA**, Hiroshi USUKI** and Naohiko SUGITA**
* Makino Milling Machine Co., Ltd.,
4023 Nakatsu, Aikawa-machi, Aiko-gun, Kanagawa 243-0303, Japan
E-mail: kajikawa@makino.co.jp
** Department of Mechanical Engineering, The University of Tokyo,
1-3-1 Hongo, Bunkyo-ku, Tokyo 113-8656, Japan

Received: 18 July 2023; Revised: 10 September 2023; Accepted: 28 September 2023

Abstract
Due to the high precision and high speed of spindles for machining centers, thermal issues cannot be avoided. The temperature rises of the spindle shaft, which is the rotating component, causes issues such as increased thermal displacement in the tool axis direction and an increase in friction torque, leading to limitations on the spindle speed. Heat removal or heat diffusion methods are effective in reducing the temperature of the spindle shaft. The former method of removing heat from the rotating shaft requires complex peripheral devices for cooling. Here, the latter method of diffusing heat is examined. Specifically, a method for reducing the temperature of the high-temperature part and the temperature difference generated in the shaft will be examined.
In order to diffuse the heat of the spindle shaft, it is necessary to increase the thermal conductivity of the shaft. In this study, highly oriented pyrolytic graphite (HOPG), which has recently attracted attention in the semiconductor field, is used for the spindle shaft instead of heat pipes (HP), which are generally used for heat diffusion. The temperatures of the rotor and bearings during rotation of the HOPG spindle shaft and the normal steel spindle shaft were measured. Under the conditions of $D_m n$ value of 1.53×10^6 mm/min, the hot part of the normal steel spindle shaft is 42°C and the generated temperature difference is 8K. On the other hand, with the HOPG shaft, it was able to reduce to 40°C and the generated temperature difference was reduced to 5K. By using a spindle shaft with high thermal conductivity by HOPG, it was found that the temperature of the high temperature part can be lowered and the temperature difference occurring in the shaft can be reduced.

Keywords: Spindle shaft, Highly Oriented Pyrolytic Graphite (HOPG), Heat Pipe (HP), Thermal conductivity, Heat diffusion, Machining center

1. Introduction

A heat remedy using a heat pipe (HP) is known as a method of diffusing the heat of the spindle shaft. A review paper by Chen et al. (2021) presents research papers by mainly Asian researchers on motor cooling for automobiles. In the paper, there are examples of heat remedies in stators, rotors and coils using HP. Besides, a review paper by Denkena et al. (2020) introduces a paper on the cooling of machine tool spindles, which is closer to the content described here. This review paper introduces examples of heat remedies for spindle motors, bearings, and rotors. It is stated that active cooling, which involves applying external cooling media such as air, oil, or coolant to the motor, is effective (Wegener et al., 2017). Next, regarding bearings, a technology for cooling the bearings using the air used in oil-air lubrication was introduced by NTN Corporation (2016). Finally, there are research reports by Li et al. (2018) and patents by Fedoseyev et al. (2014) that use the rotating shaft itself, which is the rotor, as the HP. However, it should be noted that

Paper No.23-00286
[DOI: 10.1299/jamdsm.2023jamdsm0065]

the spindle shaft of the machining center is not a solid cylindrical structure, that is, the clamping mechanism for the cutting tool is mounted inside the shaft. In other words, the shaft itself is hollow to implement other mechanisms inside, and so the shaft itself cannot be HP.

In previous studies, a method for mounting a hollow tube annular HP inside of the shaft was proposed by Hashimoto et al. (1996). The annular type of HP referred to here is an HP that is not rod-shaped but has a shape like a hollow tube, and the shaft itself can be the HP. However, research on annular HP has not been continuously reported, moreover there is no literature after 2000. Another method is to make a deep hole in the thin part of the hollow shaft and insert a thin HP. Alternatively, a patent by Mitsubishi Heavy Ind., Ltd. (1996) has been issued in the past in which a groove is provided to enclose a highly volatile liquid for heat exchange, whereas it has not been put to practical use. Although HP has a thermal conductivity of 2 000 W/mK or more, there are many restrictions to bring out its performance. For example, since the HP is an elongated cylindrical part, it is necessary to insert this cylindrical HP into a deep slot filled with glue. In such mounting, large errors occur in deep hole drilling in thin portions, thickness control of adhesive layers, and edge processing. Furthermore, due to the production of HP parts, it is practically difficult to mount in narrow places. Under these circumstances, it is necessary to investigate ways to dissipate heat from the spindle shaft without using HP.

In this study, the spindle shaft was manufactured using highly oriented pyrolytic graphite (HOPG), which is a high thermal conductivity material, instead of parts like HP. HOPG has a thermal conductivity of 1 700 W/mK, which is comparable to HP, has good manufacturability, so that it can be inserted into narrow spaces with a thin adhesive layer. In other words, depending on the design, a heat diffusion effect equivalent to HP can be secured, and a highly reliable spindle shaft can be manufactured. The temperature distribution during rotation of the HOPG spindle shaft and the normal steel shaft is measured to confirm the temperature reduction effect. In addition, the temperature of the front bearing part of the shaft and the thermal displacement in the axial direction of the tool are measured, in consequence the relationship between them is also reported.

2. Design of spindle shaft using HOPG

2.1 High thermal conductivity materials

Table 1 shows the results of investigations on materials with high thermal conductivity. The materials are arranged in descending order of thermal conductivity. Single-layer graphene (SLG) is the best thermal conductor (Balandin et al., 2008). However, the thickness of this material is only 0.33 nm, so it cannot be used as a mechanical component. The second highest thermal conductor is HOPG laminated with SLG. It is a structure in which graphene films are stacked, and the thermal conductivity of HOPG is reported to be 1 700 W/mK by Patel et al. (2012) and Sabatino et al. (2014). The material with the third highest thermal conductivity is boron arsenide with a thermal conductivity of 1 300 W/mK (Li et al., 2018). However, the material discovered in 2018 has many unclear points and the scale is less than 1mm. The fourth material is diamond, which has a high thermal conductivity ranging from 1 000 to 2 200 W/mK . However, it presents challenges in terms of size, cost, and processability.

Copper and aluminum are high thermal conductors those have long been used in machines. If copper or aluminum is used as the structural material for the spindle shaft, high thermal conductivity can be obtained without considering joining, however it does not have the necessary rigidity and hardness for the spindle shaft. Therefore, it cannot be used as a structural material, and is used as an addition to carbon steel, which is a conventional structural material. It is the same metal as the carbon steel used for the spindle shaft, and it has good workability and can be mounted in a narrow place, but the thermal conductivity of copper and aluminum is inferior to other high thermal conductors. Based on the above results, HOPG is used for the shaft as a high thermal conductor.

The reason why HOPG can be applied to spindle shafts is the size and workability of HOPG. Besides, Fig. 1 shows a photograph of a HOPG sample taken with a ballpoint pen. What should be explained is that it can be manufactured in a sufficient size. This material is laminated by the Chemical Vapor Deposition (CVD) method and can be manufactured up to a thickness of 20mm. As a material, it is manufactured as a block of 300mm x 300mm x 20mm by Thermo Graphitics Co., Ltd. (2022). Since the surface is uneven when cut from the material, cutting with a graphite processing machine is required when using it as a part.

[DOI: 10.1299/jamdsm.2023jamdsm0065]

Table 1 Thermal conductivity of materials.

Material	Thermal conductivity λ [W/mK]
Single phase graphene (SLG)	4 840-5 300 (on plane)
Highly Oriented Pyrolytic Graphite (HOPG)	1 700 (on plane), 7 (Thickness direction)
Boron arsenide	1 300
Diamond	1 000-2 200 (Kidalov et al., 2009)
Copper (C1100)	390
Aluminum (pure)	236
isotropic graphite	100-250
Carbon steel (S45C: JIS)	52

Fig. 1 HOPG sample.

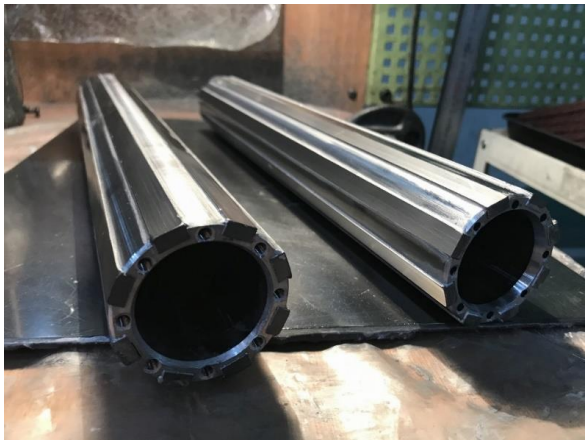

Fig. 2 HOPG bonded to the inner cylinder of the spindle shaft.

2.2 Joining HOPG and carbon steel

When using HOPG for a spindle shaft, it is first necessary to understand its mechanical properties. HOPG is brittle and does not allow mechanical joints such as bolts. In other words, it is appropriate to use HOPG by bonding to a structural material by such as adhesion. Spindle shaft materials require high toughness and threaded hole strength, and bearing fittings require a tolerance of about 1μm for cylindricity. Therefore, the structural material of the spindle shaft is conventionally used, and carbon steel is used because it can be mechanically joined and has high toughness. Therefore, the design policy of the spindle shaft was to use conventional carbon steel as a structural material and to join HOPG by adhesion.

Next, it was examined how to bond HOPG to the carbon steel. Fig. 2 shows HOPG adhered to the outer circumference of the inner cylinder of the spindle shaft. When an adhesive is used for the spindle, the adhesive must not only have high thermal conductivity, but also be excellent in water resistance and oil resistance. This is because it is assumed that the shaft will be exposed to lubricating oil and coolant. The adhesive used in the joining process of such metal parts is selected from among epoxy-based adhesives that are excellent in water resistance and oil resistance. Epoxy-based adhesives retain strength and possess corrosion resistance because epoxy resins are less prone to absorbing water or oil, and they exhibit limited susceptibility to chemical reactions.

Adhesive containing fine aluminum powder with high thermal conductivity was used for bonding HOPG. The thermal conductivity of adhesives containing fine aluminum powder is one of the highest among epoxy adhesives, but its thermal conductivity is only 1.3 W/mK (Aremco Products Inc., 2022). Therefore, a thick adhesive layer reduces the heat diffusion effect and is a value to be considered in the design of the spindle.

[DOI: 10.1299/jamdsm.2023jamdsm0065]

2.3 Verification of adhesion thickness

Consider the thickness of the adhesive layer from the design point of view. Even if HOPG with high thermal conductivity is used, it becomes a design problem if heat cannot be diffused by the adhesive. In order to quantify the effect of adhesive thickness, thermal resistance was calculated under the conditions shown in Fig. 3. As shown in the figure, the thermal resistance was obtained when two carbon steel cylinders with a thickness of 20 mm, which are close to the actual size, were bonded with an adhesive with varying thicknesses. In addition, the interfacial thermal resistance of the adhesive was added based on the literature on similar adhesives (Ogushi et al., 2015). The following thermal resistance calculation formula (1) was used for the calculation.

$$R_a = \frac{8h_{cs}}{\pi \cdot {D_{cs}}^2 \cdot \lambda_c} + \frac{4t_a}{\pi \cdot {D_{cs}}^2 \cdot \lambda_a} + \dot{R_i} * \frac{\pi \cdot {D_{cs}}^2}{4} \quad (1)$$

Where thermal resistance R_a : [K/W], thickness of adhesive layer t_a : [m], thickness of carbon steel h_{cs}=0.02 : [m], contact surface of diameter D_{cs}=0.03 : [m], thermal conductivity coefficient of carbon steel $\lambda_c = 52$: [W/mK], thermal conductivity coefficient of adhesive $\lambda_a = 1.3$: [W/mK], interfacial thermal resistance $\dot{R_i}$=1.2×10^{-5} : [m^{2}K/W].

Table 2 shows the results of calculation under the above formula under four conditions: condition A: no adhesion, B: adhesive layer 0.01 mm, C: adhesive layer 0.1 mm, and D: adhesive layer 1 mm. In the case of condition B, the thermal resistance increases by about 1% compared to condition A, which does not adhere. In the case of condition C, the thermal resistance increases by about 10%, and in the last case of condition D, the thermal resistance is more than double that of condition A, which is not adhered. To put it simply, if the adhesive layer is 1mm, the thermal resistance is equivalent to that of carbon steel with a thickness of 40mm or more. Based on the results, the thermal resistance under conditions close to the actual size is reduced to an increase of about 10%, similarly the design was performed under condition C, which limits the increase in thermal resistance to a carbon steel thickness of about 4mm. The adhesive layer thickness t_a= 0.1mm under condition C is easier to manage than the adhesive layer thickness t_a= 0.01 mm under condition B and is considered appropriate as a manufacturing tolerance.

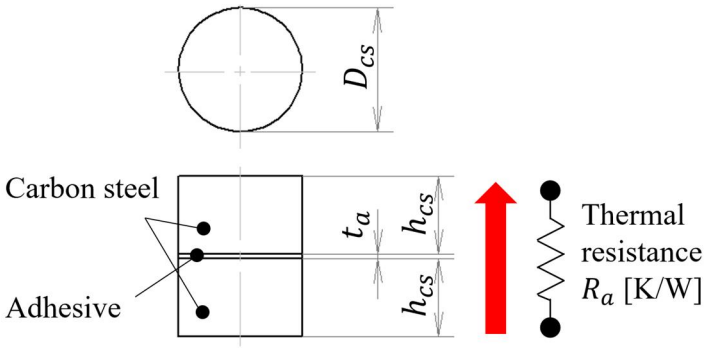

Fig. 3 Thermal resistance calculation conditions.

[DOI: 10.1299/jamdsm.2023jamdsm0065]

Table 2 Calculation results of thermal resistance.

	Adhesive layer thickness			
	A	B	C	D
$\mathbf{t_a}$ [mm]	0	0.01	0.1	1
$\mathbf{D_{cs}}$ [mm]	30			
$\boldsymbol{h_{cs}}$ [mm]	20			
$\mathbf{R_a}$ [K/W]	1.105	1.116	1.214	2.193

2.4 Spindle shaft design

Fig. 4 shows the visual indication of a spindle shaft in which HOPG is bonded to carbon steel. The spindle shaft has a three-part structure consisting of an inner cylinder, an outer cylinder, and a tapered part so that heat can be diffused from the tip of the shaft to the rear end. The gray material is carbon steel, likewise the black material is HOPG. By making the spindle shaft of one part into three parts, HOPG can be effectively placed in places that were impossible with HP. The elongated HOPG prisms are placed on the outer circumference of the shaft inner cylinder. In addition, 8 HOPG cylinders are placed at the same intervals on the tapered part and the tip of the shaft outer cylinder, which are difficult to place in the HP. Note that HOPG is an anisotropic material and has a low thermal conductivity of 7W/mK in the thickness direction. The HOPG prisms and cylinders bonded there are oriented to have high thermal conductivity in the axial and radial direction of the spindle. The reason for this orientation is to move the heat on the surface toward the center of the shaft to heat the inside to a high temperature, thereby diffusing the heat in the direction of the rotation axis.

On the other hand, separating the spindle shaft, which is normally manufactured in one piece, creates the following risks. For example, a centrifugal force or an external force applied to the shaft may cause misalignment between the split parts. Misalignment degrades the balance and accuracy of the spindle shaft, degrading spindle performance. Therefore, the inner cylinder was coated with an adhesive and inserted into the outer cylinder. Furthermore, as shown in Fig. 5, the outer cylinder and the inner cylinder are bolted so that the inner cylinder and the outer cylinder are not misaligned. Besides, the taper part is fastened to the outer cylinder with bolts, but it cannot be glued because it needs to be disassembled when replacing the bearing. Therefore, the risk of splitting was avoided by using an interference fit for the fitting of the tapered part to prevent misalignment. Fig. 6 shows the manufactured spindle shaft. The left side is a conventional spindle shaft made only of carbon steel (hereafter referred to as carbon steel shaft), and the right side is a spindle shaft with HOPG bonded to carbon steel (hereafter referred to as HOPG shaft).

Next, Fig. 7 shows the cross section of the spindle used in the verification. In the verification, the rotation axis of the spindle was installed vertically. The lower side, which is the tool side, is called the front side, likewise the upper side is called the rear side. The spindle used was a general machining center spindle. The spindle shaft in the figure is a HOPG shaft. The bearing arrangement consists of two rows of fixed-position preloaded angular bearings on the front side, and one row of angular bearings on the rear side across the rotor. The spindle housing has three cooling grooves for stator cooling, front bearing cooling and rear bearing cooling. The cooling oil flowing through these grooves is supplied by a temperature control unit. The temperature control unit controls the return oil temperature to keep it at a stable temperature for the machine. For the convenience of verification, unlike the actual spindle, it does not have a tool clamping unit. Implement a sensor bar for temperature measurement instead of the tool clamp unit. Table 3 shows a summary of spindle specifications such as the inner diameter of the front bearing.

[DOI: 10.1299/jamdsm.2023jamdsm0065]

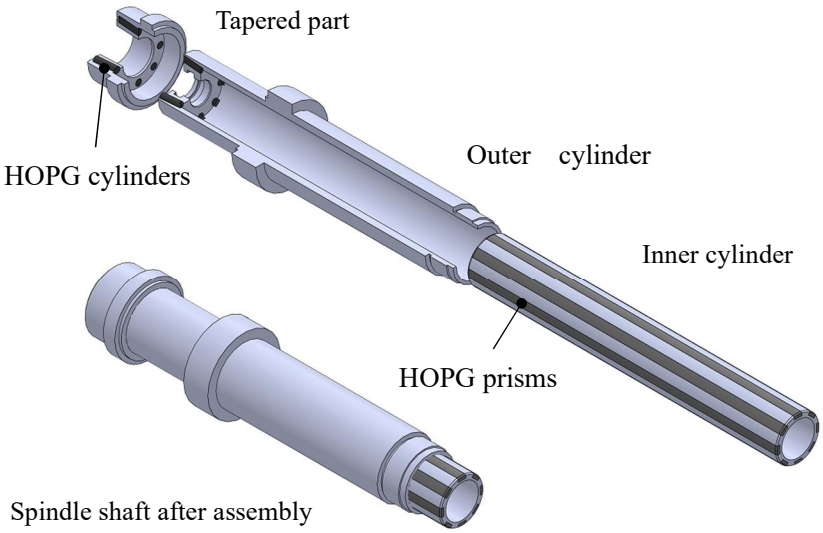

Fig. 4 Visual indication of a spindle shaft in which HOPG is bonded to carbon steel.

Fig. 5 front side bolts of the outer cylinder.

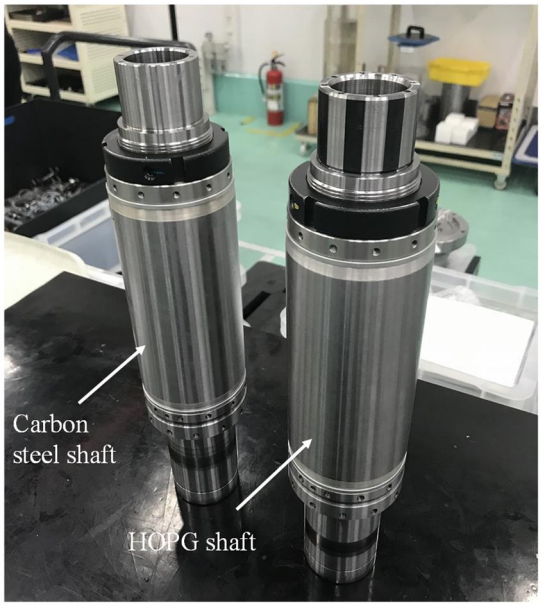

Fig. 6 Appearance of the manufactured spindle shaft.

[DOI: 10.1299/jamdsm.2023jamdsm0065]

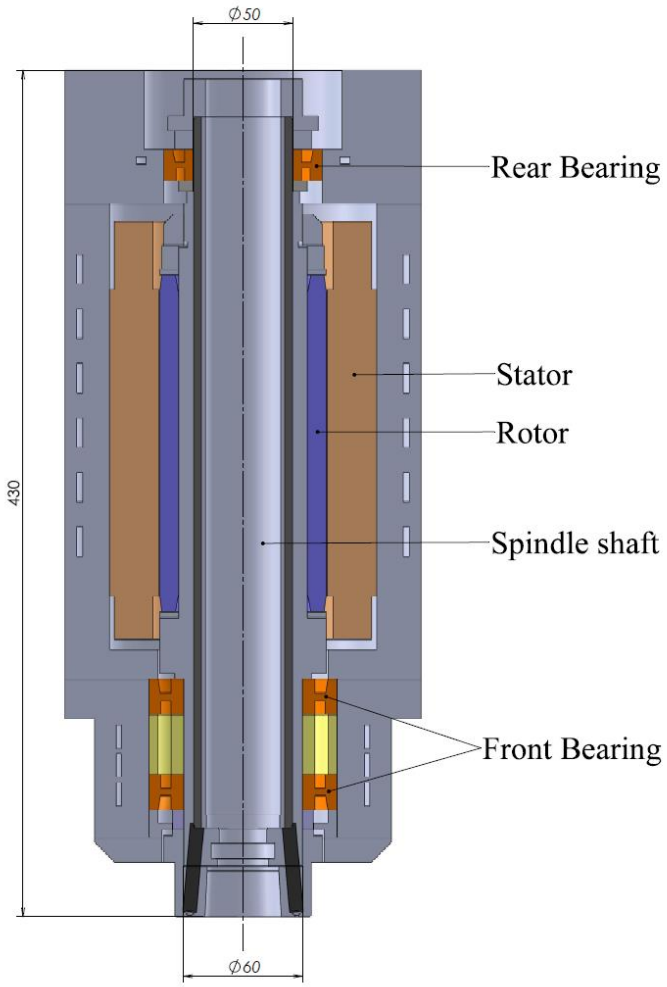

Fig. 7 Spindle cross section.

Table 3 Spindle specifications.

Specifications	**Contents**
Tool interface	HSK-F63 size
Spindle motor type (Squirrel-cage induction motor)	Built-in type/Two steps electric change over
Motor power	11kW/Continuous rating
Spindle speed	200～20 000min^{-1}
$D_m n$ value	1.53×10^6 mm/min
Front bearing inner diameter	60mm
Rear bearing inner diameter	50mm
Preload of the front bearing	Rigid preload
Lubrication	Oil air lubrication
Cooling	Cooling jacket
Remarks	Equipped with sensor unit

[DOI: 10.1299/jamdsm.2023jamdsm0065]

3. Temperature measurement of the spindle shaft

3.1 Sensor bar for the temperature measurement

Fig. 8 shows a cross-sectional view of the spindle shaft with the sensor bar inserted. A sensor bar for temperature measurement shown in the figure was press-fitted into the spindle shaft. The temperature measuring part of the K-type thermocouple is glued onto the resin ring attached to the outer circumference of the sensor bar, and the part of the sensor comes into close contact with the inner diameter side of the spindle shaft by press-fitting. In this way, it was possible to place the thermocouples as close as possible to the rotor and bearings, which are heat sources. Three temperature measurement points are provided on the shaft front bearing, rotor, and rear bearing. A plastic wire guide is press-fitted into the sensor bar to protect the thermocouple and transmitter wires.

3.2 Temperature measurement conditions

Table 4 shows the spindle rotation conditions. The purpose was to measure the temperature in the high speed range with a spindle speed of 10 000 min^{-1} or more. The spindle speed was set to increase stepwise from 500 min^{-1} to 20 000 min^{-1}. In condition a), it was rotated at 500min^{-1} for 40 minutes. The reason for rotating at low speed before rotating at high speed is to stabilize the lubricating state of the bearing. In conditions b) to e), the rotation speed was increased by 2 500 min^{-1} from 10 000 min^{-1} to 17 500 min^{-1} every 20 minutes, and in condition f), it was rotated at the maximum speed of 20 000 min^{-1} for 60 minutes. After that, it was stopped at condition g). Under this spindle rotation condition, the temperature of the spindle shaft and the temperature of the front housing were respectively taken into the data logger from the receiver and the thermocouple and measured. The temperature measurements were conducted under no machining load, specifically during the no-load rotation condition. The verification was performed at least twice to confirm that the temperature was reproducible.

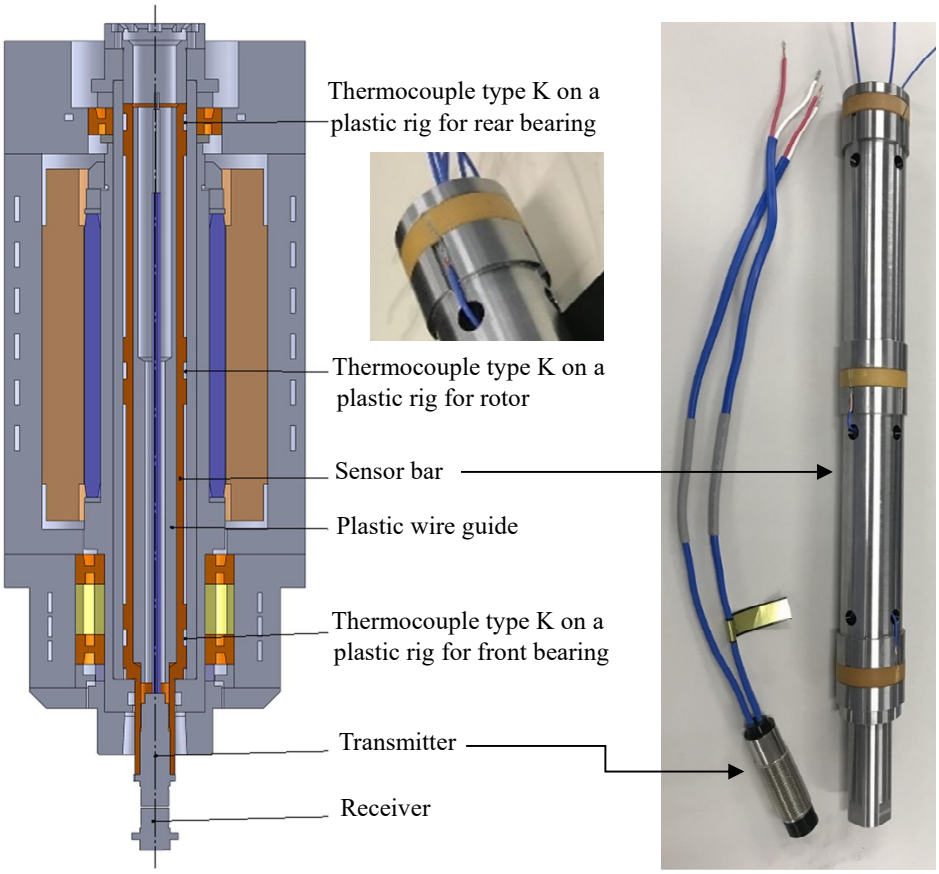

Fig. 8 Sensor bar for the temperature measurement of spindle shaft.

[DOI: 10.1299/jamdsm.2023jamdsm0065]

Table 4 The spindle rotation conditions.

Conditions	Spindle speed	Time	$D_m n$
	[min^{-1}]	[min]	[mm/min]
a)	500	40	38
b)	10 000	20	0.767×10^6
c)	12 500	20	0.958×10^6
d)	15 000	20	1.15×10^6
e)	17 500	20	1.34×10^6
f)	20 000	60	1.53×10^6
g)	0	-	0

3.3 Temperature measurement results

Fig. 9 shows the results of time and temperature measurements during rotation with a carbon steel shaft. Black indicates the rotor, red indicates the front bearing, blue indicates the rear bearing, and orange indicates the front housing temperature. First, the temperature of the rotor shown in black, which is the highest in the spindle shaft, will be described. The black rotor temperatures under conditions at the ends of each stage were 38.5°C, 38°C, 35°C, 35°C and 42°C, respectively. The reason why the temperature decreases when the rotation speed is increased to 12500, 15000 and 17500 rotations is that the rotor temperature has no positive correlation with the rotation speed. Next, the temperature difference between rotor, front bearing, and rear bearing at three locations on the spindle shaft was checked. The temperature differences at the ends of each stage were 15K, 12K, 8K, 5K and 8K, respectively. From this result, it can be seen that a maximum temperature difference of 15K occurs in the spindle shaft, and heat is not diffused.

On the other hand, Fig. 10 shows the measurement results of time and temperature when performing rotation with the HOPG shaft. By using HOPG, the thermal conductivity of the spindle shaft is increased, the maximum temperature of the shaft is lowered under all conditions, furthermore the temperature difference is small. First, the temperature of the black rotor of the spindle shaft was 34°C, 34°C, 33°C, 34°C and 40°C under conditions at the ends of each stage, respectively. The maximum temperature of the HOPG shaft could be lowered by 1K to 4.5K. Next, the temperature difference between rotor, front bearing, and rear bearing at three locations on the spindle shaft is 7K, 6K, 3.5K, 2Kand 3K under conditions at the ends of each stage, respectively. The temperature difference at three points on the HOPG shaft decreased from 3K to 8K. It can be seen from this that by using HOPG, there is only a maximum temperature difference of 7 K, and the heat is more diffused than with a carbon steel shaft.

Consider the temperature reduction and heat diffusion of the HOPG shaft. The highest rotor temperature is lowered under all conditions, and so it can be said that there is an effect of reducing the temperature of the highest part. The significant aspect to focus on is the heat diffusion effect, as replacing the carbon steel shaft with an HOPG shaft reduced the temperature difference by up to 8K. Due to the heat diffusion effect of the HOPG shaft, the temperature difference at maximum speed is only 3K.

[DOI: 10.1299/jamdsm.2023jamdsm0065]

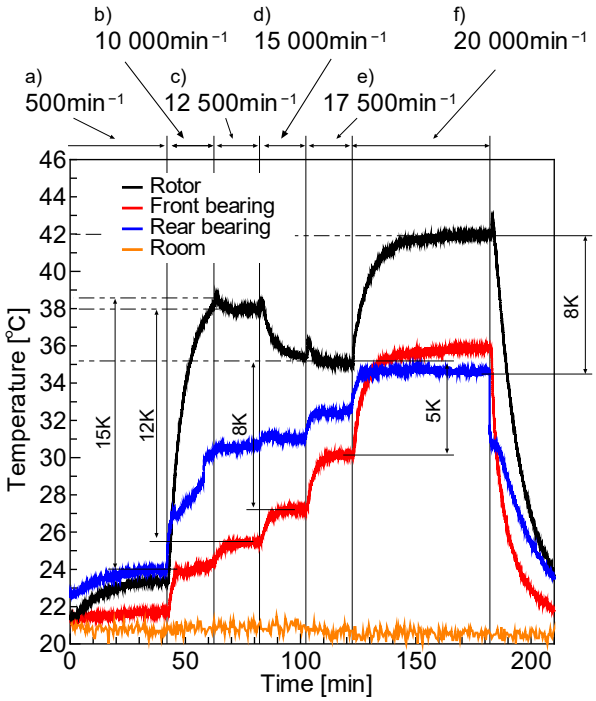

Fig. 9 Temperature measurement result of the carbon steel shaft.

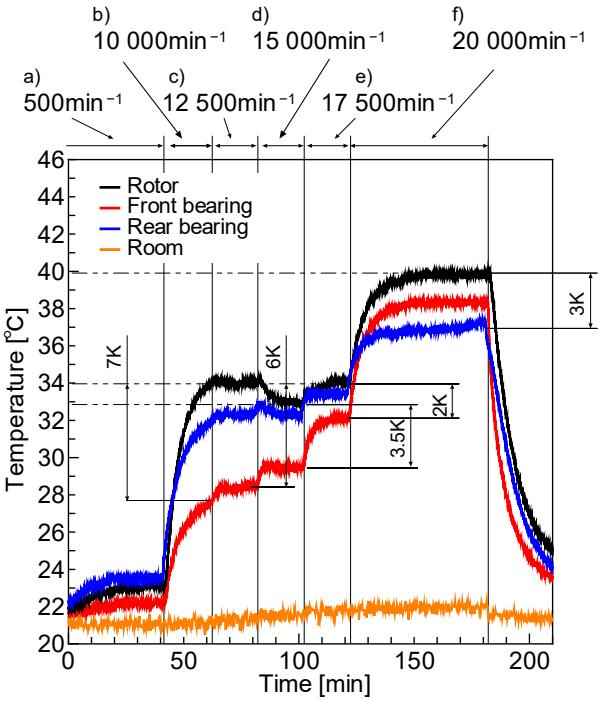

Fig. 10 Temperature measurement result of the HOPG shaft.

4. Relationship between thermal displacement and front bearing temperature

4.1 Measurement of thermal displacement

The thermal displacement of a spindle supported by a front bearing with a fixed position preload is believed to be proportional to the front bearing temperature. In a spindle simply supported by a front bearing, if the temperature up to the tip of the spindle shaft is the same as the temperature of the front bearing, The thermal displacement is calculated by multiplying the temperature rise at the front bearing section by the linear expansion coefficient. In order to confirm the thermal displacement of the spindle and the temperature of the front bearing, the thermal displacement of the spindle was measured under the same conditions as above.

The measurement method is shown in cross-sectional views and photographs in Fig. 11 a) and Fig. 11 b). The thermal displacement of the spindle was measured with a non-contact eddy-current displacement sensor fixed to the front housing. Since the thermal displacement is measured from the front housing, which supports the outer ring of the front bearing, it reduces the impact of thermal displacement from the spindle housing, which tends to become hotter due to the stator. The distance from the spindle housing to the sensor measurement position was 100 mm, and the temperature of the experimental environment was controlled at 21°C ± 0.5°C. A typical thermal displacement measurement involves clamping a test bar onto a spindle shaft and measuring the displacement of its tip. In contrast, the thermal displacement was measured at the end face of the shaft because the tool could not be clamped with the verification spindle.

[DOI: 10.1299/jamdsm.2023jamdsm0065]

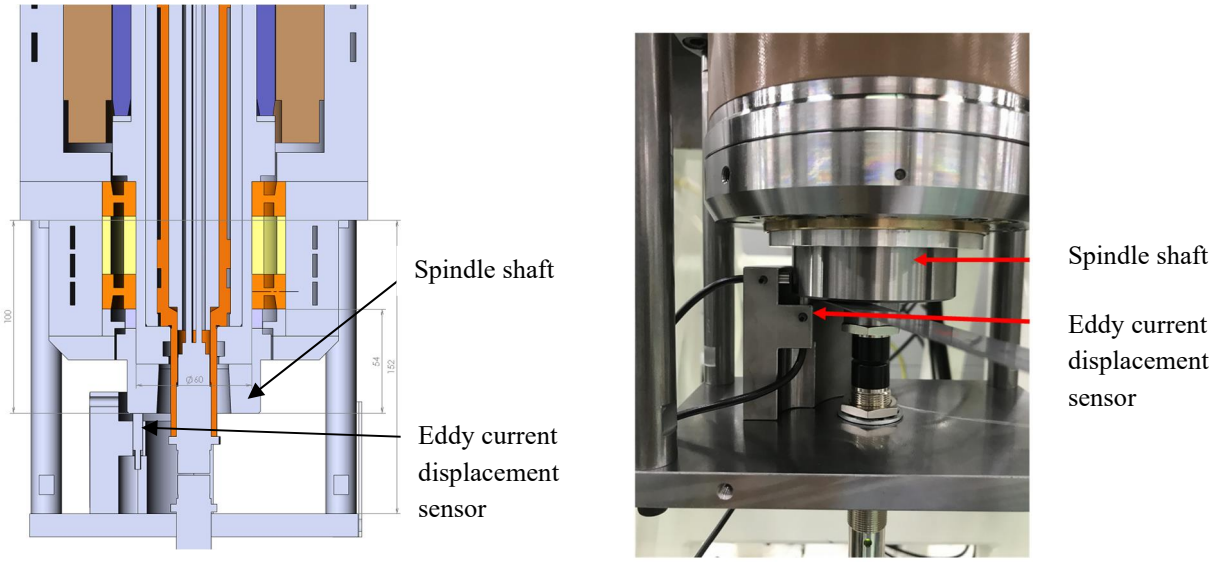

a) Schematic b) Photo

Fig. 11 Spindle thermal displacement measurement.

4.2 Relationship between thermal displacement and front bearing temperature

The thermal displacement measurement results are shown in Fig. 12. The horizontal axis is time, and the vertical axis is the thermal displacement of the end surface of the spindle shaft. Thermal displacement is measured directly at the end face of the spindle shaft. It should be noted that the amount of displacement decreases for about 10 seconds immediately after increasing the spindle speed. Since this decrease in displacement is short-lived, it is considered not due to thermal deformation, but due to external force accompanying an increase in spindle speed. As a basis, the reduced displacement in the axial direction is calculated. The shaft radially expands due to centrifugal force during spindle speed change, which reduces the axial displacement of the shaft. From formula (2) for calculating the displacement of the hollow rotary disk, the radial expansion displacement due to centrifugal force is 1.2 μm when shifting from condition e) to f). Also, the amount of reduction in axial displacement is 0.3 μm from formula (3). However, when shifting from condition e) to condition f), the amount of reduction in axial displacement is about 1 μm, and there are other factors that reduce the amount of axial displacement due to external forces. One of them is the change in the bearing contact angle. As the contact angle decreases, the axial displacement of the bearing decreases. Therefore, thermal displacement does not include the amount of displacement that decreases immediately after the rotation speed is increased. In addition, when the thermal displacement under each condition is read as the amount of increased displacement after shifting speed, it becomes 0.6 μm, 0.9 μm, 2.4 μm and 4.6 μm under conditions c), d), e) and f), respectively.

$$u_{r2} = \frac{1}{4E}\left((1-\upsilon)r_2^2 + (3+\upsilon)r_1^2\right)\rho r_2(\varpi_2^2 - \varpi_1^2) \tag{2}$$

where radial expansion displacement u_{r2}:[mm], Outer diameter and inner diameter of the shaft are r_2=0.04 : [m], r_1=0.025 : [m], Young's modulus E＝2.06×10^{11} : [Pa], Poisson's ratio υ=0.3, Density ρ=7 800: [kg/m^3], Angular velocity before shifting ϖ_1: [rad/s], Angular velocity after shifting ϖ_2: [rad/s] .

$$u_x = \frac{v \cdot Dist}{r_2} u_{r2} \tag{3}$$

However, the axial displacement is u_x:[mm], and the distance from the front bearing to the spindle end face is Dist=54: [mm].

[DOI: 10.1299/jamdsm.2023jamdsm0065]

Next, Fig. 13 shows the results of plotting the temperature rise of the front bearing on the vertical axis. The front bearing temperature rise is simply the bearing temperature minus the initial temperature. On the vertical axis of the figure, the thermal displacement using the calculation formula (4) from the temperature rise is added. The calculated thermal displacements from conditions b) to c), d), e) and f) are 0.7μm, 0.8μm, 1.7μm and 4.1μm, respectively, which are in good agreement with the previously measured thermal displacements.

$$\Delta x = \alpha_{st} * \mathrm{Dist} * \Delta t \tag{4}$$

However, the thermal displacement is Δx:[mm], the linear expansion coefficient is α_{st}=11.7:[10^{-6}/K], and the temperature rise is Δt:[K].

Let us now consider the amount of thermal displacement when changing from the initial state to the maximum speed. The thermal displacement from the initial state is 8.9 μm in Fig. 12, and the thermal displacement calculated from the bearing temperature is 11 μm in Fig 13. The actual amount of thermal displacement is 2.1μm smaller than the thermal displacement calculated from the bearing temperature. This decrease in displacement is believed to result from deformation caused by external forces immediately after rotation. Deformations due to external forces may include axial displacement due to centrifugal forces and changes in the bearing's contact angle.

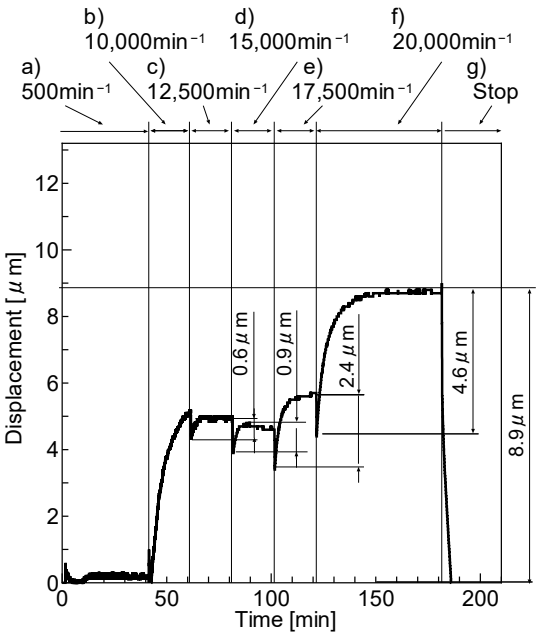

Fig. 12 Measurement result of the thermal displacement.

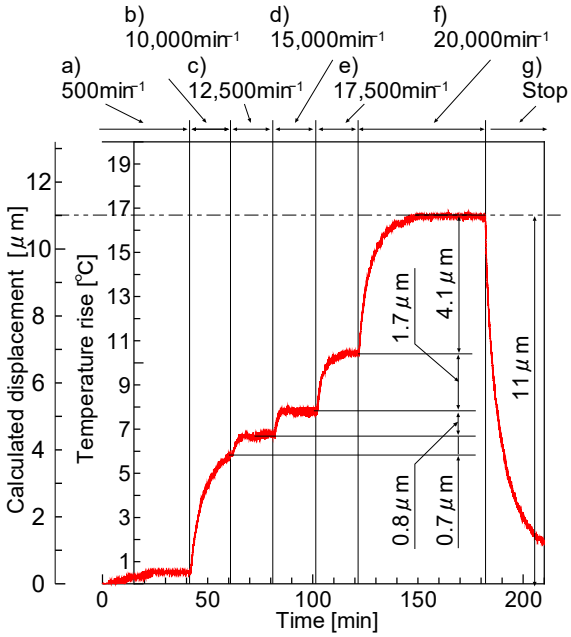

Fig. 13 Temperature rise of the front bearing and the calculated displacement.

5. Discussion

5.1 Heat diffusion of spindle shaft by HOPG

In this study, HOPG was used for the spindle shaft of machining centers for the first time. There are examples of HOPG being applied to molds as a patent by Thermo Graphitics Co., Ltd., (2018), however there are no examples of its application to machine tools. Until now, HP has generally been used to improve the thermal conductivity of spindle shafts. Table 5 shows a comparison table between HP and HOPG. It is the result of comparing each item of design, ease of manufacture, thermal conductivity, and actual heat diffusion with ○ ×. What can be understood here is that while HP possesses extremely high thermal conductivity, its drawbacks are often regarded as being challenging to design and manufacture.

[DOI: 10.1299/jamdsm.2023jamdsm0065]

Table 5 Comparison between heat pipe and highly oriented pyrolytic graphite.

	Heat pipe (HP)	Highly Oriented Pyrolytic Graphite (HOPG)
Design	× Limited in shape, directional	○ Anisotropic material
Manufacturability	× Drilling deep and narrow hole	△ Use glue
Heat transfer coefficient	◎ More than 2 000 W/mK	○ 1 700W/mK
Actual heat spreading performance	○	○

HOPG, on the other hand, is easy to design and easy to build. Taking advantage of this degree of design freedom, the challenges of HOPG's brittleness and low rigidity were able to be addressed by using carbon steel for the shaft's outer diameter and incorporating HOPG internally. In addition, it was easy to manage the adhesive thickness of the placed HOPG, and it was easy to assemble. In this verification, it was possible to process with HOPG with precision close to that of metal, and Fitting tolerance was able to set with a gap of 0.1 mm. Furthermore, HOPG could be placed in a narrow space at the end of the spindle. It was found that HOPG can also be applied to parts where space is limited, such as spindle shafts. From these points, it is thought that the application of HOPG to machine tools as an alternative to HP will be considered in the future.

The purpose of installing HOPG was to diffuse the heat from the high temperature part of the spindle shaft to the entire shaft and lower the temperature. The results show that the HOPG shaft can reduce the rotor temperature, which is the highest temperature, by a maximum of 5K, and by 2K at maximum speed. An even greater effect is the heat diffusion effect of HOPG. The carbon steel shaft generated a maximum temperature difference of 15K, although the HOPG shaft reduced the temperature difference to 7K. From the above results, it has become clear that using HOPG in the spindle shaft lowers the temperature of the high-temperature parts and reduces the temperature difference that occurs between the rotor, front bearing, and rear bearing.

5.2 Temperature of front bearing and accuracy of spindle

Let us consider the relationship between the accuracy of the spindle supported by the front bearing and the temperature of the shaft bearing section. Regarding accuracy, verification revealed that the value obtained by multiplying the temperature rise in the bearing section by the linear expansion coefficient of the shaft has a positive correlation with thermal displacement. In other words, it has become clear that as the temperature of the bearing section increases, spindle accuracy decreases, as the temperature decreases, spindle accuracy improves.

In the verification, the main factor was the temperature of the rotor section, which is at the highest temperature, so by using a HOPG shaft that enhances the overall heat diffusion effect, the temperature of the bearing section increased. In short, the result was that the accuracy was lowered by promoting the heat diffusion. Therefore, when increasing the overall heat diffusion effect, it is important to confirm in advance that the bearing section will be at the highest temperature.

It is easy to predict that accuracy will be improved by using a HOPG shaft in a spindle where the bearing part is the hottest. Also, if the heat quantified by the bearing and the rotor is uncertain, it is important to consider thermal diffusion that can cope with the case where the rotor temperature is high.

[DOI: 10.1299/jamdsm.2023jamdsm0065]

6. Conclusion

The spindle shaft with high thermal conductivity was manufactured by HOPG, furthermore a rotation test similar to that of a normal carbon steel spindle shaft was performed. The temperature distribution of the spindle shaft was measured, and the following conclusions were obtained.

1. It was found that the temperature at the high-temperature part of the spindle shaft during rotation was 40°C at $D_m n$ value of 1.53×10^6 mm/min, which could be reduced by 2K due to the high thermal conductivity of HOPG.
2. It was found that the temperature difference caused by the HOPG shaft when rotating at $D_m n$ value of 1.53×10^6 mm/min is only 3K.
3. Heat spreading by the HOPG shaft can reduce the temperature and temperature difference in the hot part of the shaft, however the overall temperature will increase due to the inability to remove heat. In order to further increase the accuracy and speed of the spindle, remedies to remove heat are thought to be effective.

We measured the thermal displacement of the spindle and obtained the following findings.

It was confirmed that there is a strong positive correlation between the temperature of the front bearing part of the spindle shaft and the thermal displacement of the spindle. The measured thermal displacement of the spindle was several μm smaller than the thermal displacement calculated from the bearing temperature of the spindle shaft. This amount of decrease is considered to be the amount of decrease caused by deformation due to external force immediately after rotation.

Acknowledgments

I would like to thank Makino Milling Machine Co., Ltd. for their financial support throughout the process of writing the thesis.

References

Aremco Products Inc., High Performance Epoxies 568 Aluminum-Filled, 1:1, High Bond Strength, Excellent Thermal Conductivity (online), available from <https://www.aremco.com/conductive-compounds/>, (accessed on 01 September, 2023).

Balandin, A.A., Ghosh, S., Bao, W., Calizo, I., Teweldebrhan, D., Miao, F. and Lau, C. N., Superior thermal conductivity of single-layer graphene, Nano letters, Vol. 8, No. 3 (2008), pp. 902-907.

Chen, Z., Yu, Z., Fu, J. and Liu, B., Study of heat pipe in motor cooling: A review, E3S Web of Conferences ICMEE 2021, (2021), DOI:10.1051/e3sconf/202126101009.

Denkena, B., Bergmann, B. and Klemme, H., Cooling of motor spindles-a review, The International Journal of Advanced Manufacturing Technology, Vol. 110, (2020), pp. 3273-3294.

Fedoseyev, L., Pearce, E.M., Applied for by Tesla Motors, Inc., Rotor assembly with heat pipe cooling system, Patent no. US 2014/0368064 A1, (2013).

Hashimoto, R., Mizuta, K., Itani, H., Kura, K. and Takahashi, Y., Heat transport performance of rotating heat pipes installed in high-speed spindle, Mitsubishi Heavy Industries, Ltd. Technical Review Vol. 33, No. 2 (1996), pp. 88-92.

Kidalov, S. V. and Shakhov, F. M., Thermal conductivity of diamond composites, Materials Vol. 2, No. 4 (2009), pp. 2467-2495.

Li S., Zheng, Q., Lv, Y., Liu, X., Wang, X., Huang, P. Y., Cahill, D.G. and Lv, B., High thermal conductivity in cubic boron arsenide crystals, Science (American Association for the Advancement of Science), Vol. 361, No. 6402

[DOI: 10.1299/jamdsm.2023jamdsm0065]

(2018), pp. 579-581.

Li, F., Gao, J., Shi, X., Liang, F. and Zhu, K., Experimental investigation of single loop thermosyphons utilized in motorized spindle shaft cooling, Applied Thermal Engineering Vol. 134, (2018), pp. 229-237.

Nakamura, K., Mitsubishi Heavy Ind Ltd., Spindle, Japanese patent JPH10113845A (1996).

NTN Corporation, TECHNICAL REVIEW No.84 Special Issue: Green Energy Products and Machine Tool / Manufacturing Technology (online), available from <https://www.ntnglobal.com/en/products/review/index.html>, (accessed on 01 September, 2023).

Ogushi, T., Yanaura, S., Watanabe, S. and Hirata, T., Thermal conductivity measurement method for isotropic conductive adhesives, Netsu bussei Vol. 28, No. 1 (2015), pp. 22-28.

Patel, A,N., Collignon, M.G., O'Connell, M.A., Hung, W.O., McKelvey, K., Macpherson, J.V. and Unwin, P. R., A New View of Electrochemistry at Highly Oriented Pyrolytic Graphite, Journal of the American Chemical Society, Vol. 134, No. 49 (2012), pp. 20117-20130.

Sabatino, D. and Yoder, K., Pyrolytic graphite heat sinks: A study of circuit board applications, IEEE Transactions on Components, Packaging and Manufacturing Technology, Vol. 4, No. 6 (2014), pp. 999-1009.

Thermo Graphitics Co., Ltd., HOPG (online), available from <http://www.thermo-graphitics.com/index.html>, (accessed on 01 September, 2023).

Thermo Graphitics Co., Ltd., Japanese patent JP6376812 B2, (2018).

Wegener, K., Mayr, J., Merklein, M., Behrens, B. A., Aoyama, T., Sulitka, M., Fleischer, J., Groche, P., Kaftanoglu, B. and Möhring, H. C., Fluid elements in machine tools, CIRP Annals Vol. 66, No. 2 (2017), pp. 611-634.

[DOI: 10.1299/jamdsm.2023jamdsm0065]